Critical relationships in nonviscous systems with proportional damping

Mario Lázaro[a,b,*], Luis M. García-Raffi[b]

[a] *Department of Continuum Mechanics and Theory of Structures*
Universitat Politècnica de València 46022 Valencia, Spain
[b] *Instituto de Matemática Pura y Aplicada (IUMPA)*
Universitat Politècnica de València 46022 Valencia, Spain

Abstract

Materials with time-dependent dissipative behavior currently play an important role in the design of new mechanisms for vibration control in civil, automotive, aeronautical and mechanical engineering. Damping forces are assumed to depend on the past history of the velocity response via convolution integrals over multiple exponential hereditary kernels. Hence, the computational complexity increases both in time and frequency domain with respect to the widely used viscous models. The derivations of this article are carried out under the hypothesis of nonviscous proportional damping, that is, the time-dependent damping matrix becomes diagonal in the modal space of the undamped system. In this context, the damping parameters, which control the behaviour of dissipative forces, will be considered as variable. Critical manifolds can be defined as hypersurfaces in the domain of the damping parameters, which represent boundaries between oscillatory and non-oscillatory motion. In particular, critical manifolds of two parameters are the so-called critical curves. In this paper a new method to obtain critical curves in proportionally damped nonviscous multiple degree-of-freedom systems is presented. It is proved that the conditions of critical damping lead to relationships that enables an analitical determination of such critical curves, in parametric form. In addtion, it is demonstrated that modal critical regions arise as the interesection of the critical curves. The proposed method is validated through two numerical examples involving discrete and continuous system with generalized proportional damping.

Keywords:
viscoelastic sytems, nonviscous systems, critical damping, eigenvalues, proportional damping

1. Introduction

In this paper, nonviscously damped linear dynamical systems are under study. Viscoelastic (or nonviscous) damping models are extensively used to describe the behavior of time-dependent materials. Damping forces are expressed as a convolution integral in order to represent the dependency on the history of velocity response. The equations of motion can be written as [1]

$$\mathbf{M}\ddot{\mathbf{u}} + \int_{-\infty}^{t} \boldsymbol{\mathcal{G}}(t-\tau)\,\dot{\mathbf{u}}\,\mathrm{d}\tau + \mathbf{K}\mathbf{u} = \mathfrak{f}(t) \tag{1}$$

where $\mathbf{u}(t) \in \mathbb{R}^n$ denotes the degrees of freedom (dof), $\mathbf{M}$, $\mathbf{K} \in \mathbb{R}^{n\times n}$ are the mass and stiffness matrices, assumed to be positive definite and positive semidefinite, respectively; $\boldsymbol{\mathcal{G}}(t) \in \mathbb{R}^{n\times n}$ is the viscoelastic damping matrix, expressed as function of time, assumed symmetric as well. Viscous damping arises when the hereditary functions degenerate to the Dirac's delta function, $\boldsymbol{\mathcal{G}}(t) \equiv \mathbf{C}\,\delta(t)$, where $\mathbf{C}$ is the viscous damping matrix. Eq. (1) yields then

$$\mathbf{M}\ddot{\mathbf{u}} + \mathbf{C}\dot{\mathbf{u}} + \mathbf{K}\mathbf{u} = \mathfrak{f}(t) \tag{2}$$

*Corresponding author. Tel +34 963877000 (Ext. 76732)
Email addresses: malana@mes.upv.es (Mario Lázaro), lmgarcia@mat.upv.es (Luis M. García-Raffi)

Considering solutions of the form $\mathbf{u}(t) = \boldsymbol{u}\, e^{st}$ in Eq. (1), we find the eigenvalue problem

$$\left[s^2\mathbf{M} + s\mathbf{G}(s) + \mathbf{K}\right] \boldsymbol{u} \equiv \mathbf{D}(s)\, \boldsymbol{u} = \mathbf{0} \tag{3}$$

where $\mathbf{G}(s) = \mathcal{L}\{\boldsymbol{\mathcal{G}}(t)\} \in \mathbb{C}^{n\times n}$ is the damping matrix, $\mathbf{D}(s)$ is the dynamical stiffness matrix or transcendental matrix and s is the Laplace parameter. Eigenvalues of Eq. (3) are the roots of equation

$$\det\left[\mathbf{D}(s)\right] = 0 \tag{4}$$

The time-domain response can be written in terms of these eigenvalues. It is known that conjugate-complex eigenmodes lead to oscillatory motion with decay in amplitude directly proportional to the real part of s. Lightly damped nonviscous systems present as many conjugate-complex pairs modes as the number of degrees of freedom. In addition, there exist certain number of real modes associated to the nonviscous nature of hereditary kernels [2, 3]. The system root locus strongly depends on the damping parameters, such that certain combination of them can result in some (or all) eigenvalue(s) falling on the real axis. losing its oscillatory nature and becoming overdamped. In the damping parameters domain, boundaries can be established between oscillatory and nonoscillatory induced motion. Such limits define mathematically the concept of critical damping. Since the dissipative model in general depends on a high number of parameters, we can talk about critical hypersurfaces or manifolds. However, in practice, these are usually represented in 2D, leading to the so-called critical curves. Lázaro [4] showed that critical surfaces of nonviscous systems can theoretically be determined after elimination of the Laplace parameter s from

A certain combination of the parameters can result in an eigenvalue falling on the real axis

$$\det\left[\mathbf{D}(s)\right] = 0 \quad , \qquad \frac{\partial}{\partial s}\det\left[\mathbf{D}(s)\right] = 0 \tag{5}$$

Most of the research on critical damping has been carried out so far in the context of purely viscous forces. Therefore, it is worth reviewing the main milestones in this field. Using minimax principle, Duffin [5] studied critical conditions in linear dynamical systems. Sufficient conditions for underdamping were derived by Nicholson [6] studying eigenvalue bounds. These results were enhanced by Müller [7], proposing conditions for subcritical damping in all modes. Inman and Andry [8] proposed sufficient conditions for critical damping studying the definiteness of the system matrices. Barkwell and Lancaster [9] solved some shortcomings presented in the Inman and Andry model. Barkwell and Lancaster [9] studied critical damping in gyroscopic systems deriving new conditions for criticality. Beskos and Boley [10] proved for viscous systems mathematical conditions to find critical relationships in terms of the s-derivative of the system determinant. These conditions, although mathematically consistent, were in practice inappropriate for medium or large systems, due to the need to find the analytical expression of the system determinant, as well as its derivative. The procedure was substantially improved from a computational point of view by Papargyri-Beskou and Beskos [11], proving that critical manifolds can be approached considering that critical eigenvalues are $s = -\omega_j,\ 1 \le j \le n$, where ω_j denotes the jth natural undamped frequency.

Viscous forces are characterized by being proportional to the velocity of the response. In the frequency domain, this fact simplifies the study of the critical damping conditions with respect to the use of nonviscous damping. The introduction of viscoelastic dissipative forces increases the mathematical complexity of the problem, since the damping matrix becomes now function of the frequency. Even for single degree-of-freedom systems, the order of the characteristic equation increases with the number of hereditary kernels, something that makes it impossible to solve in the variable s in the general case of N kernels, for obvious reasons. Therefore, the first attempts to enlighten the conditions of critical damping started with Muravyov and Hutton [12] and Adhikari [13], addressing the problem with just one hereditary kernel with exponential nature and discussing the real-complex nature of the roots of the resulting third order characteristic polynomial. Müller [14] studied the oscillatory nature of eigenvalues for single degree-of-freedom systems with nonviscous damping model based on a Zener 3–parameter model. Muravyov [15] studied conditions for overdamped motion in the context of forced viscoelastic beams. Lázaro [16] studied the critical damping of single degree-of-freedom oscillators for multiple hereditary kernels. Critical curves for viscoelastic beams

have been recently studied by Pierro [17] where the eigenvalues are analytically obtained and their nature (real or complex) studied. The method is interesting because explores the method for two hereditary kernels with the Cardano formulas (arising four-degree polynomials), but with the disadvantage that cannot be extended for more kernels. With respect to critical damping of models based on fractional derivative, references in the bibliography are very rare. As far as the authors' knowledge goes, the only work of relative relevance is a recent article by Wang [18] where a study of the fractional orders compatible with critical solutions is addressed. In the ref. [4], the second condition of Eqs. (5) was derived for nonviscous systems and both equations were used to study critical surfaces in viscoelastic systems. In fact, in this work a new numerical method based on the transformation of these two relationships into a system of differential equations was proposed. It turns out that this procedure is not operative in practice for larger systems in which to obtain analytical expressions of the determinant becomes highly inefficient due to its computational complexity. In the ref. [19], an approach for multiple degree-of-freedom systems but restricted to models with a single hereditary kernel was proposed.

In this article we investigate the critical surfaces of classical or proportional non-viscous systems, without limitation in the structure of hereditary functions, i.e. any number of exponential kernels are admitted. Real-life structures with classical damping have proved to be very useful for modal analysis, since the damping matrix can be completely diagonalized under the undamped modal matrix transformation. The conditions to be verified by the system matrices for this purpose were first studied by Rayleigh [20], establishing the proportionality relationships between the damping matrix and the mass and stiffness matrices. The concept of proportionality was extended by Caughey and O'Kelly [21] and finally generalized by Adhikari[22]. Additionally, for nonvsicous damping, Adhikari [23] gave necessary and sufficient conditions on the time-domain damping matrix to present classical normal modes. Proportional damping in viscoelastic systems allows the study of complex problems such as those involving the response in structures with temperature-dependent behavior [24, 25]. In the particular case of the study of critical damping, the only two references found for systems with multiple degrees of freedom (Pierro [17], Wang et al. [18]) consider proportional damping. The reason: a general numerical method to find critical curves in viscoelastic structures is not available yet. The existing investigations have proposed solutions for specific cases before addressing the general problem, which would consider no restriction in the number of degrees of freedom, neither in proportionality of the damping matrix or in the number of hereditary kernels.

In control of dynamical systems, it is essential to know how to adjust the damping parameters of a multiple degree-of-freedom system to ensure the system evolves as designed. In particular, there are many applications in vibration control where the goal is to find out overdamping conditions. This article presents a new methodology to determine the critical relationships in nonviscously damped proportional systems with no restriction on the number of hereditary kernels. The capability of the system to become diagonal in the undamped modal space enables the decomposition of the determinant of the system into a product of the decoupled modal equations and hence critical relations between the parameters can analytically be evaluated. The critical curves can be determined for each mode dividing the parametric domain in overdamping regions. These regions may be overlapped, something that physically is interpreted as multiple overdamped modes. The theoretical results are validated through two numerical examples. In the first example a 4-degree-of-freedom discrete system with damping matrix proportional to the stiffness matrix is studied. In the second example, a continuous system with generalized proportional damping is analyzed.

2. Theoretical background and critical relations for proportional damping

In this paper, damping based on the Biot's [26] model will be considered. In general, the nonviscous damping matrix can be written as the superposition of N hereditary exponential functions which can be expressed both in time and frequency domain as

$$\boldsymbol{\mathcal{G}}(t) = \sum_{k=1}^{N} \mathbf{C}_k \, \mu_k \, e^{-\mu_k t} \quad , \quad \mathbf{G}(s) = \mathcal{L}\{\boldsymbol{\mathcal{G}}(t)\} = \sum_{k=1}^{N} \frac{\mu_k}{s+\mu_k} \mathbf{C}_k \tag{6}$$

where $\mu_k > 0$, $1 \leq k \leq N$ represent the relaxation (or nonviscous) parameters and $\mathbf{C}_k \in \mathbb{R}^{n\times n}$ are the symmetric damping matrices of the limit viscous model, obtained in the limit case as the relaxation parameters tend to infinite, that is

$$\sum_{k=1}^{N} \mathbf{C}_k = \lim_{\mu_1 \ldots \mu_N \to \infty} \mathbf{G}(s) \tag{7}$$

The damping model, governed by the s-dependent matrix $\mathbf{G}(s)$, depends on a set of damping parameters that control dissipative behavior. Thus, the symmetric damping model presented in (6) depends at most on $p_{\max} = N + Nn(n+1)/2$ independent parameters. Indeed, $n(n+1)/2$ possible independent entries within each $\mathbf{C}_k, 1 \leq k \leq N$ plus the nonviscous parameters μ_k. Thus, the complete set of parameters can be listed as

$$\bigcup_{k=1}^{N} \{\mu_k,\ C_{11}^{(k)}\ ,\ C_{12}^{(k)}\ ,\ \ldots\ ,\ C_{n,n-1}^{(k)}\ ,\ C_{nn}^{(k)}\} \tag{8}$$

where $C_{ij}^{(k)} = C_{ji}^{(k)}$ is the ij-entree of $\mathbf{C}_k$, assumed symmetric. Real applications depend in general on far fewer parameters, say $p << p_{\max}$. The coefficients μ_k control the time– and frequency–dependence of the damping model while the spatial location and the level of damping are modeled via the matrices $\mathbf{C}_k$.

The main objective of this article is to present a procedure to obtain relationships between parameters (called critical curves) that enables drawing of the thresholds between oscillatory and non-oscillatory behavior for proportionally damped systems. At this point, it becomes necessary to revisit the concept of proportional damping and the definition of undamped modal space, because the forthcoming developments are closely related to them. Assume that $\omega_j \in \mathbb{R}$ and $\boldsymbol{\phi}_j \in \mathbb{R}^n$, are the natural frequencies and undamped eigenvectors, respectively. It is well known that they are related through

$$\mathbf{K}\boldsymbol{\phi}_j = \omega_j^2 \mathbf{M}\boldsymbol{\phi}_j\ ,\ 1 \leq j \leq n \tag{9}$$

The eigenvectors $\boldsymbol{\phi}_j$ can be arranged as the columns of the modal matrix

$$\boldsymbol{\Phi} = [\boldsymbol{\phi}_1, \ldots, \boldsymbol{\phi}_n] \in \mathbb{R}^{n\times n} \tag{10}$$

Assuming that there are not repeated natural frequencies, the eigenvectors can be mass-normalized using the biorthogonality relations

$$\boldsymbol{\phi}_j^T \mathbf{M}\boldsymbol{\phi}_k = \delta_{jk}\ ,\quad \boldsymbol{\phi}_j^T \mathbf{K}\boldsymbol{\phi}_k = \omega_j^2\, \delta_{jk}\ ,\quad \boldsymbol{\phi}_j^T \mathbf{G}(s)\boldsymbol{\phi}_k = g_{jk}(s) \tag{11}$$

where δ_{jk} is the Kronecker delta. If the off-diagonal terms of the damping matrix vanish, that is $g_{jk}(s) = g_{jj}(s)\,\delta_{jk}$, then the nonviscous damping matrix $\boldsymbol{\mathcal{G}}(t)$ is said to be proportional (or classical). Adhikari [23] proved that nonviscously damped systems present classical normal modes if and only if the following relationship between mass, stiffness and damping matrices hold

$$\mathbf{K}\,\mathbf{M}^{-1}\,\boldsymbol{\mathcal{G}}(t) = \boldsymbol{\mathcal{G}}(t)\mathbf{M}^{-1}\,\mathbf{K} \tag{12}$$

Assuming the above form for $\boldsymbol{\mathcal{G}}(t)$, then these conditions are satisfied provided that

$$\mathbf{K}\,\mathbf{M}^{-1}\,\mathbf{C}_k = \mathbf{C}_k\mathbf{M}^{-1}\,\mathbf{K}\quad ,\quad \forall\ k = 1, \ldots, N \tag{13}$$

This condition holds provided that the Rayleigh proportionality relationship is verified for every viscous damping matrix, $\mathbf{C}_k$, i.e.

$$\mathbf{C}_k = a_k\,\mathbf{M} + b_k\,\mathbf{K} \tag{14}$$

The concept of proportionality was extended by Caughey and O'Kelly [21], proving that the following representation of the damping matrix $\mathbf{C}_k$

$$\mathbf{C}_k = \mathbf{M} \sum_{j=0}^{m-1} a_j\ \left(\mathbf{M}^{-1}\,\mathbf{K}\right)^j \tag{15}$$

is the necessary and sufficient condition for existence of classical normal modes provided that there are not repeated eigenvalues. This result was later generalized by Adhikari [22], proving that viscoelastic systems with positive definite matrices can be totally decoupled in the undamped space if and only if the damping matrices can be represented by

$$\mathbf{C}_k = \mathbf{M}\, f_1(\mathbf{M}^{-1}\mathbf{K}) + \mathbf{K}\, f_2(\mathbf{K}^{-1}\mathbf{M}) \quad \text{or} \quad \mathbf{C}_k = f_3(\mathbf{K}\mathbf{M}^{-1})\,\mathbf{M} + f_4(\mathbf{M}\mathbf{K}^{-1})\,\mathbf{K} \tag{16}$$

where $f_i(z)$ are smooth analytic functions in the neighborhood of all the eigenvalues of their argument matrices. In other words, the Caughey series associated to this generalized proportional damping has infinite terms (Taylor series expansion of such analytic functions). The assumption of generalized proportional damping can be specially useful when modal damping ratios present such a variation that requires more sophisticated functions. Adhikari [22] proposed a method of identification specifically constructed for this proportionally damped structures. In the context of the current paper, some coefficients a_j of Eq. (15) will be non-fixed parameters. In the most general case, the functions $f_i(z)$ will depend on certain set of non fixed parameters. The proposed approach enables construction of relationships between pairs of these free parameters that establish the thresholds between overdamped and underdamped induced vibrations.

According to the general results about critical damping in nonviscous systems obtained by Lázaro [4], any real eigenvalue $s \in \mathbb{R}^-$ of a nonviscously damped system is critical if and only if

$$\det\left[\mathbf{D}(s)\right] = 0 \quad , \qquad \frac{\partial}{\partial s}\det\left[\mathbf{D}(s)\right] = 0 \tag{17}$$

With a proportional damping model, the dynamic stiffness matrix in the modal space

$$\mathbf{d}(s) = \mathbf{\Phi}^T\,\mathbf{D}(s)\,\mathbf{\Phi} = s^2\mathbf{I}_n + s\,\mathbf{g}(s) + \mathbf{\Omega}^2 \ \in \mathbb{C}^{n\times n} \tag{18}$$

becomes diagonal. Above $\mathbf{I}_n$ denotes the nth order identity matrix, $\mathbf{g}(s) = \mathbf{\Phi}^T\,\mathbf{G}(s)\,\mathbf{\Phi}$ and $\mathbf{\Omega} = \mathrm{diag}\,[\omega_1, \ldots, \omega_n]$. Thus Eqs. (17) can be rewritten in the modal space in an equivalent form as

$$\det\left[\mathbf{d}(s)\right] = \prod_{k=1}^{n} d_{kk}(s) = \prod_{k=1}^{n}\left(s^2 + s\,g_{kk}(s) + \omega_k^2\right) = 0 \tag{19}$$

$$\frac{\partial}{\partial s}\det\left[\mathbf{d}(s)\right] = \sum_{l=1}^{n} d'_{ll}(s) \prod_{\substack{k=1\\k\neq l}}^{n} d_{kk}(s) = 0 \tag{20}$$

where $(\bullet)' = \partial/\partial s$. Assume that $s \in \mathbb{R}^-$ is a real negative eigenvalue of the jth mode, with undamped eigenvector $\boldsymbol{\phi}_j$, then $d_{jj}(s) = \boldsymbol{\phi}_j^T\mathbf{D}(s)\boldsymbol{\phi}_j$=0. If, in addition, the equation $d'_{jj}(s) = 0$ is also verified, then both equations (19) and (20) hold simultaneously and $s \in \mathbb{R}^-$ is critical or, in other words, the associated set of damping parameters lie on a critical manifold. Therefore, the two equations

$$d_{jj}(s) = \boldsymbol{\phi}_j^T\mathbf{D}(s)\boldsymbol{\phi}_j \quad , \qquad d'_{jj}(s) = \boldsymbol{\phi}_j^T\frac{\partial\mathbf{D}}{\partial s}\boldsymbol{\phi}_j = 0 \tag{21}$$

define mathematically the critical relationships for the jth mode. If $\mathbf{G}(s)$ is formed by N hereditary kernels, then equations $d_{jj}(s) = 0$ and $d'_{jj}(s) = 0$ can be reduced to two polynomials of order $N+2$ and $N+1$, respectivaly. The critical manifolds arise after deleting the parameter s from both equations. However, this procedure can not be carried out in practice when the degree of the lowest order resulting polynomial is greater than 4, that is $N > 3$. Even in cases where analytical solutions do exist, the resulting radical-based expressions cannot be manipulated for study due to complexity [12, 13, 17]. Thus, instead of approaching the solution from a perspective based on removing s from both expressions, the problem will be addressed considering s as an independent parameter.

Let us demonstrate that if $s \in \mathbb{R}^-$ is a critical eigenvalue associated to jth mode, then $s \leq -\omega_j$. Indeed, the two equations (21) can be written as

$$\boldsymbol{\phi}_j^T \mathbf{D}(s) \boldsymbol{\phi}_j = s^2 + s\, g_{jj}(s) + \omega_j^2 = 0 \tag{22}$$

$$\boldsymbol{\phi}_j^T \frac{\partial \mathbf{D}}{\partial s} \boldsymbol{\phi}_j = 2s + g_{jj}(s) + s\, g'_{jj}(s) = 0 \tag{23}$$

Now, dividing Eq. (22) by s^2 and Eq. (23) by s and substracting, it yields

$$-1 + \frac{\omega_j^2}{s^2} - g'_{jj}(s) = 0 \tag{24}$$

Using the properties of the Laplace transform, we have $g'_{jj}(s) = -\mathcal{L}\{t\, \boldsymbol{\mathcal{G}}(t)\} < 0$ for any $s < 0$. Hence, rewritting Eq. (24)

$$1 - \frac{\omega_j^2}{s^2} = \mathcal{L}\{t\, \boldsymbol{\mathcal{G}}(t)\} \geq 0 \tag{25}$$

which leads to $s \leq -\omega_j$ for negative critical eigenvalues (associated to the jth mode). Furthermore, the equality $s = -\omega_j$ only holds for viscously damped systems for which $g'_{jj}(s) \equiv 0$. Thus, if a dimensionless parameter is defined as $\alpha = -\omega_j / s$, it is straightforward that the values of α are bounded by the interval $0 < \alpha \leq 1$. Hence, in Eqs. (22) and (23) the damping parameters are now unknowns and α can be read as an independent parameter. According to the general form of $\mathbf{G}(s)$, the expressions of $g_{jj}(s)$ and $g'_{jj}(s)$ are, namely

$$g_{jj}(s) = \sum_{k=1}^{N} \frac{\mu_k}{s + \mu_k} \boldsymbol{\phi}_j^T \mathbf{C}_k \boldsymbol{\phi}_j \ , \quad g'_{jj}(s) = -\sum_{k=1}^{N} \frac{\mu_k}{(s + \mu_k)^2} \boldsymbol{\phi}_j^T \mathbf{C}_k \boldsymbol{\phi}_j \tag{26}$$

After plugging these expressions into Eqs. (22) and (23), it yields

$$s^2 + \sum_{k=1}^{N} \frac{s\mu_k}{s + \mu_k} \boldsymbol{\phi}_j^T \mathbf{C}_k \boldsymbol{\phi}_j = 0 \tag{27}$$

$$2s + \sum_{k=1}^{N} \frac{\mu_k^2}{(s + \mu_k)^2} \boldsymbol{\phi}_j^T \mathbf{C}_k \boldsymbol{\phi}_j = 0 \tag{28}$$

Substituting $s = -\omega_j / \alpha$, and after some simplifications it yields

$$\sum_{k=1}^{N} \frac{\alpha}{\alpha - \omega_j / \mu_k} \frac{\boldsymbol{\phi}_j^T \mathbf{C}_k \boldsymbol{\phi}_j}{\omega_j} = \frac{1 + \alpha^2}{\alpha} \tag{29}$$

$$\sum_{k=1}^{N} \left(\frac{\alpha}{\alpha - \omega_j / \mu_k} \right)^2 \frac{\boldsymbol{\phi}_j^T \mathbf{C}_k \boldsymbol{\phi}_j}{\omega_j} = \frac{2}{\alpha} \tag{30}$$

These two expressions summarize the main contribution of this paper. Indeed, choosing any pair of parameters, within the set of Eq. (8), and fixing the rest, the two above expressions define analytically a parametric curve in terms of $\alpha \in (0, 1]$. This curve represents the critical values of the chosen parameters for which the mode j is critically damped. In other words, they define a boundary between undercritical and overcritical induced-motion regions, for the jth mode. Since the system can be completely decoupled due to its proportionality, critical curves can be drawn separately for each mode, giving rise to a family of overdamped regions which may be overlapped. This overlapping has a physical meaning, representing combination of damping parameters which induce multiple-modes overdamping, something that will be visualized in the numerical examples.

In the following examples the results obtained will be validated and the corresponding critical curves will be depicted for the different pairs of parameters that can be formed.

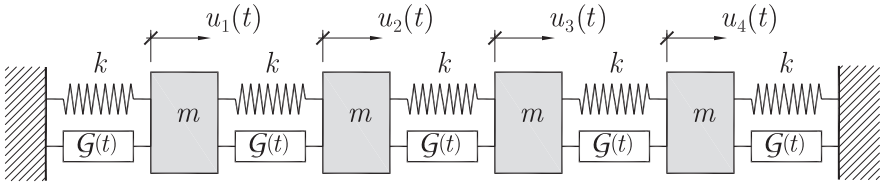

Figure 1: Example 1: The four degrees-of-freedom discrete system with proportional damping. $\mathcal{G}(t) = c_1\mu_1 e^{-\mu_1 t} + c_2\mu_2 e^{-\mu_2 t}$ represents the hereditary function and c_1, c_2, μ_1, μ_2 are the damping parameters. The numerical values of the mass and rigidity are $m = 10$ kg, $k = 10^3$ N/m respectively. The critical damping curves will be presented in nondimensional form using the reference frequency $\omega_r = \sqrt{k/m}$ and defining the nonviscous and viscous ratios, say $\nu_i = \omega_r/\mu_i$, $\zeta_i = c_i/2m\omega_r$, respectively.

3. Numerical examples

3.1. Example 1: Discrete systems

The proposed method will be validated throught two numerical examples. In the first one, a mass-lumped dynamical system with $n = 4$ degrees of freedom (dof) is analyzed. Fig. 1 shows the structural configuration with masses $m = 10$ kg and linear rigidities $k = 10^3$ N/m together with a nonviscous damper characterized by the hereditary function

$$\mathcal{G}(t) = c_1\,\mu_1\,e^{-\mu_1 t} + c_2\,\mu_2\,e^{-\mu_2 t} \tag{31}$$

where c_1, c_2 are the viscous damping coefficients and μ_1, μ_2 are the relaxation parameters. The results of the proposed method will be studied in terms of the (dimensionless) viscous and nonviscous ratios defined respectively as

$$\zeta_i = \frac{c_i}{2m\omega_r} \quad , \quad \nu_i = \frac{\omega_r}{\mu_i} \quad , \quad i = 1, 2 \tag{32}$$

where $\omega_r = \sqrt{k/m}$ is a reference frequency. The mass matrix of the system is $\mathbf{M} = m\mathbf{I}_4$ and the stiffness matrix becomes

$$\mathbf{K} = k \begin{bmatrix} 2 & -1 & 0 & 0 \\ -1 & 2 & -1 & 0 \\ 0 & -1 & 2 & -1 \\ 0 & 0 & -1 & 2 \end{bmatrix} \tag{33}$$

and, consequently, the damping matrix is $\mathbf{G}(s) = G(s)\,\mathbf{K}/k$, where $G(s) = \mathcal{L}\{\mathcal{G}(t)\} = c_1\mu_1/(s + \mu_1) + c_2\mu_2/(s + \mu_2)$. Hence both viscous damping matrices, say $\mathbf{C}_1 = c_1\mathbf{K}/k$, $\mathbf{C}_2 = c_2\mathbf{K}/k$, are proportional to the stiffness matrix leading to a classically damped system. Using the modal relations, Eqs (29) and (30) can be written as

$$\mathcal{R}_{1j}(\alpha)\,\zeta_1 + \mathcal{R}_{2j}(\alpha)\,\zeta_2 = U_j(\alpha) \tag{34}$$

$$\mathcal{R}^2_{1j}(\alpha)\,\zeta_1 + \mathcal{R}^2_{2j}(\alpha)\,\zeta_2 = V_j(\alpha) \tag{35}$$

where

$$\mathcal{R}_{1j}(\alpha) = \frac{\alpha}{\alpha - \nu_1\frac{\omega_j}{\omega_r}} \quad , \quad \mathcal{R}_{2j}(\alpha) = \frac{\alpha}{\alpha - \nu_2\frac{\omega_j}{\omega_r}} \tag{36}$$

and

$$U_j(\alpha) = \frac{1 + \alpha^2}{2\alpha}\left(\frac{\omega_r}{\omega_j}\right) \quad , \quad V_j(\alpha) = \frac{1}{\alpha}\left(\frac{\omega_r}{\omega_j}\right) \tag{37}$$

According to the derived theory, the critical curves can independently be determined resolving the damping parameters from Eqs. (34) and (35) for each mode j, $1 \le j \le n$. Any pair of parameters within the set $\{\zeta_1, \zeta_2, \nu_1, \nu_2\}$ can be found analytically from Eqs (36) as functions of the critical parameter α. In this example, two families of critical curves will be studied:

- Case 1: critical curves between the two nonviscous ratios

$$\{\nu_1^{(j)}(\alpha), \nu_2^{(j)}(\alpha),\ 0 < \alpha \leq 1,\ 1 \leq j \leq n\}$$

- Case 2: critical curves between both viscous and nonviscous ratios of the first kernel

$$\{\zeta_1^{(j)}(\alpha), \nu_1^{(j)}(\alpha)\ 0 < \alpha \leq 1,\ 1 \leq j \leq n\}$$

.

In the Case 1, the main goal is to solve for $\nu_1^{(j)}(\alpha)$ and $\nu_2^{(j)}(\alpha)$ from equations (34) and (35). Firstly, two independent quadratic equations in terms of $\mathcal{R}_{1j}$ and $\mathcal{R}_{2j}$ can be obtained, yielding

$$\zeta_1(\zeta_1+\zeta_2)\,\mathcal{R}_{1j}^2 - 2\zeta_1 U_j(\alpha)\,\mathcal{R}_{1j} + U_j^2(\alpha) - V_j(\alpha) = 0 \tag{38}$$

$$\zeta_2(\zeta_1+\zeta_2)\,\mathcal{R}_{2j}^2 - 2\zeta_2 U_j(\alpha)\,\mathcal{R}_{2j} + U_j^2(\alpha) - V_j(\alpha) = 0 \tag{39}$$

with roots

$$\mathcal{R}_{1j}(\alpha) = \frac{\zeta_1 U_j(\alpha) \pm \sqrt{\zeta_1\zeta_2\left[(\zeta_1+\zeta_2)V_j(\alpha) - U_j^2(\alpha)\right]}}{\zeta_1(\zeta_1+\zeta_2)} \tag{40}$$

$$\mathcal{R}_{2j}(\alpha) = \frac{\zeta_2 U_j(\alpha) \mp \sqrt{\zeta_1\zeta_2\left[(\zeta_1+\zeta_2)V_j(\alpha) - U_j^2(\alpha)\right]}}{\zeta_2(\zeta_1+\zeta_2)} \tag{41}$$

where the dependence on α has already been highlighted. Now, from Eq. (36), the closed-form expressions of $\nu_1^{(j)}(\alpha)$ and $\nu_2^{(j)}(\alpha)$ are respectively

$$\nu_1^{(j)}(\alpha) = \alpha\frac{\mathcal{R}_{1j}(\alpha)-1}{\mathcal{R}_{1j}(\alpha)} \quad , \quad \nu_2^{(j)}(\alpha) = \alpha\frac{\mathcal{R}_{2j}(\alpha)-1}{\mathcal{R}_{2j}(\alpha)} \tag{42}$$

where $\mathcal{R}_{1j}(\alpha)$ and $\mathcal{R}_{1j}(\alpha)$ are given by the corresponding α-dependent expressions of Eqs. (40) and (41).

The so-determined parametric curves have been plotted in Fig. 2, where the modal critical curves have been depicted with four different colours. According to the theory, such curves should exactly capture the boundaries between exact overdamped regions. In order to contrast the results, the visible region of the damping parameters, i.e. $10^{-3} \leq \nu_1, \nu_2 \leq 10^2$, has been sampled using a grid of 400×400 points. For each point, the damping model is fixed and the eigenvalues of the system can be found, so that the number of overdamped and underdamped modes can be counted. The gray scale of each point is directly related to the number of overdamped modes associated to the point. Fig. 2 shows that there exist combination of damping parameters that lead even to a total overdamping (four overdamped modes). On the other side, non gray-shaded areas refers to underdamped modes. The fit between the curves obtained and the shaded areas is perfect since the proposed approach is exact.

In addition, three different points (A, B and C) have been placed in the parameter domain. These three points represent three particular damping states and according to their location it can be predicted that (i) for point A all four modes are overdamped, (ii) point B is on (approximately) the intersection of two critical curves so that not only modes 3 and 4 will be overdamped but they will be critical and the associated eigenvalues will have double multiplicity. And (iii) point C is located within the overdamping region of the first mode, so all other modes have oscillatory eigenvalues. These results can be checked in the list of eigenvalues shown in Table 1 where four roots are shown for each mode because the damping model has two exponential kernels, giving rise to two nonviscous eigenvalues.

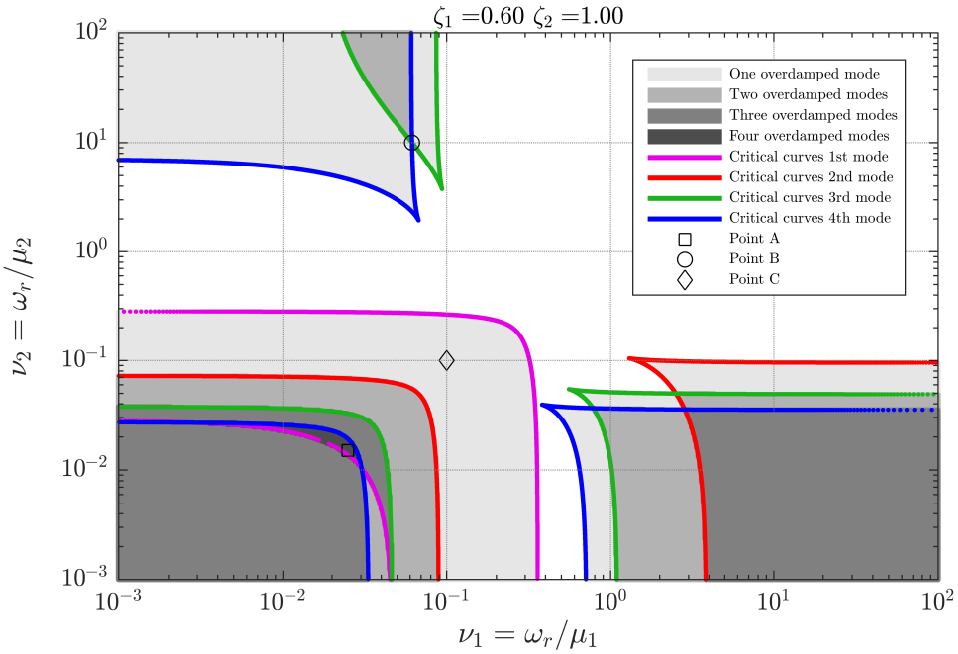

Figure 2: Example 1 (Case 1): Critical curves between nonviscous ratios $\nu_1^{(j)}(\alpha)$ and $\nu_2^{(j)}(\alpha)$. Shaded region represents exact overdamped regions. The gray scale refers to the number of overdamped modes. Color curves (magenta,red,green and blue) represent the critical curves determined with the proposed method for the four modes $j = 1, 2, 3, 4$ respectively

The second case of study deals with critical curves of viscous and nonviscous ratios corresponding to the same kernel (in this case, the first one), i.e. $\{\zeta_1^{(j)}(\alpha), \nu_1^{(j)}(\alpha)\}$. After some straight operations in Eqs (34) and (34), it yields

$$\zeta_1^{(j)}(\alpha) = \frac{[U_j(\alpha) - \zeta_2 \mathcal{R}_{2j}(\alpha)]^2}{V_j(\alpha) - \zeta_2 \mathcal{R}_{2j}^2(\alpha)} \tag{43}$$

$$\mathcal{R}_{1j}(\alpha) = \frac{V_j(\alpha) - \zeta_2 \mathcal{R}_{2j}^2(\alpha)}{U_j(\alpha) - \zeta_2 \mathcal{R}_{2j}(\alpha)} \tag{44}$$

where, as before, $\nu_1^{(j)}(\alpha)$ can be found from the above expression of $\mathcal{R}_{1j}(\alpha)$ as

$$\nu_1^{(j)}(\alpha) = \alpha \frac{\mathcal{R}_{1j}(\alpha) - 1}{\mathcal{R}_{1j}(\alpha)} = \alpha \frac{V_j(\alpha) - U_j(\alpha) + \zeta_2 \mathcal{R}_{2j}(\alpha)\,[1 - \mathcal{R}_{2j}(\alpha)]}{V_j(\alpha) - \zeta_2 \mathcal{R}_{2j}(\alpha)^2} \tag{45}$$

By sweeping out the interval $0 < \alpha \leq 1$, the curves $\{\zeta_1^{(j)}(\alpha), \nu_1^{(j)}(\alpha)\}$ can be drawn for each mode. In Fig. 3 (as in Fig. 2) only the traces of the curves within the physically possible ranges of the parameters have been plotted although negative values are also possible but physically impossible in a context of purely dissipative model. In the Case 2, it is not possible to obtain complex values since no square roots can be found in Eqs. (43) and (44), something that indeed occurs in case 1, in Eqs (40) and (41). As before, the solution of the modal characteristic polynomial has been found for each one of the 400×400 points of the grid and the gray-scale shows the number of overdamped modes in Fig. 3. It can be noted that, there exist regions where different modes are simultaneously damped. In this case, the eigenvalues associated to other three paraticular examples (points D, E and F) have also been determined in Table 1, highlighting the fact that, again, the prediction about what modes are overdamped still holds.

	Mode 1	Mode 2	Mode 3	Mode 4
Point A	$-659,022+0,000i$	$-639,041+0,000i$	$-614,858+0,000i$	$-596,280+0,000i$
	$-395,130+0,000i$	$-378,960+0,000i$	$-347,377+0,000i$	$-296,095+0,000i$
	$-6,462+0,000i$	$-45,306+0,000i$	$-101,202+0,000i$	$-171,098+0,000i$
	$-6,053+0,000i$	$-3,359+0,000i$	$-3,230+0,000i$	$-3,194+0,000i$
Point B	$-157,377+0,000i$	$-143,508+0,000i$	$-120,837+0,000i$	$-74,841+0,000i$
	$-2,446+6,477i$	$-9,381+10,133i$	$-20,828+0,000i$	$-74,590+0,000i$
	$-2,446-6,477i$	$-9,381-10,133i$	$-20,607+0,000i$	$-12,841+0,000i$
	$-0,824+0,000i$	$-0,822+0,000i$	$-0,821+0,000i$	$-0,821+0,000i$
Point C	$-100,000+0,000i$	$-100,000+0,000i$	$-100,000+0,000i$	$-48,446+96,392i$
	$-85,833+0,000i$	$-48,373+43,654i$	$-48,430+77,394i$	$-48,446-96,392i$
	$-9,465+0,000i$	$-48,373-43,654i$	$-48,430-77,394i$	$-100,000+0,000i$
	$-4,701+0,000i$	$-3,255+0,000i$	$-3,141+0,000i$	$-3,109+0,000i$
Point D	$-992,317+0,000i$	$-971,770+0,000i$	$-945,445+0,000i$	$-923,324+0,000i$
	$-191,622+0,000i$	$-155,191+0,000i$	$-126,007+76,865i$	$-137,075+110,686i$
	$-12,961+0,000i$	$-70,437+0,000i$	$-126,007-76,865i$	$-137,075-110,686i$
	$-3,100+0,000i$	$-2,602+0,000i$	$-2,542+0,000i$	$-2,525+0,000i$
Point E	$-192,060+0,000i$	$-167,244+0,000i$	$-103,486+0,000i$	$-94,776+65,411i$
	$-32,288+0,000i$	$-30,430+11,295i$	$-81,764+0,000i$	$-94,776-65,411i$
	$-4,493+4,569i$	$-30,430-11,295i$	$-43,322+0,000i$	$-39,134+0,000i$
	$-4,493-4,569i$	$-5,229+0,000i$	$-4,761+0,000i$	$-4,648+0,000i$
Point F	$-4.922,410+0,000i$	$-4.706,450+0,000i$	$-4.406,170+0,000i$	$-4.123,350+0,000i$
	$-185,657+0,000i$	$-246,550+61,111i$	$-560,115+0,000i$	$-848,841+0,000i$
	$-91,478+0,000i$	$-246,550-61,111i$	$-233,261+0,000i$	$-227,351+0,000i$
	$-0,457+0,000i$	$-0,455+0,000i$	$-0,455+0,000i$	$-0,455+0,000i$

Table 1: Example 1 (Case 1 and 2): results of eigenvalues for each point (A, B, C, D, E and F) shown in Figs. 2 and 3

3.2. Example 2: Continuous system

In this example, a continuous system consisting of a cantilever beam with a generalized proportional damping model is considered. The structural model is a $l = 5$ m long beam with 20 two-nodes Euler-Bernoulli-type finite elements with three degrees of freedom per node. The Young modulus $E = 210$ GPa and density $\rho = 7.85$ t/m^3. Mechanical properties of the cross section are $EI = 224$ kNm^2 and a mass per unit of length of $m = \rho A = 0.0628$ t/m.

The damping matrix will be assumed under a generalized porportional model [22] described above, with a mathematical expression of the form given by Eq. (16). This type of model has the advantage of ensuring that the viscous modal damping ratios describe a preset pattern as long as this can be described with analytical functions. In this example the time-domain damping matrix will be written as function of two kernels

$$\boldsymbol{\mathcal{G}}(t) = \mathbf{C}_1\,\mu_1\,e^{-\mu_1 t} + \mathbf{C}_2\,\mu_2\,e^{-\mu_2 t} \tag{46}$$

The first hereditary kernel is controlled by the viscous damping matrix $\mathbf{C}_1$ which will be assumed to be proportional to the mass matrix as

$$\mathbf{C}_1 = 2\,\zeta\,\omega_r\mathbf{M} \tag{47}$$

where $\omega_r = \sqrt{EI/ml^4}$ is a reference frequency and ζ is a dimensionless damping parameter that measures the dissipative intensity of the first kernel. The second viscous matrix $\mathbf{C}_2$ will be taken as

$$\mathbf{C}_2 = 2\mathbf{M}\left[\xi_0\,\omega_r\,\sqrt{\mathbf{M}^{-1}\mathbf{K}} + \lambda\xi_\infty\,\mathbf{M}^{-1}\mathbf{K}\right]\left[\omega_r\mathbf{I}_n + \lambda\,\sqrt{\mathbf{M}^{-1}\mathbf{K}}\right]^{-1} \tag{48}$$

where ξ_0, ξ_∞ and λ are the three independent parameters which establish the pattern of the viscous damping ratios associated to this kernel. Both $\mathbf{C}_1$ and $\mathbf{C}_2$ become diagonal in the modal space, the corresponding

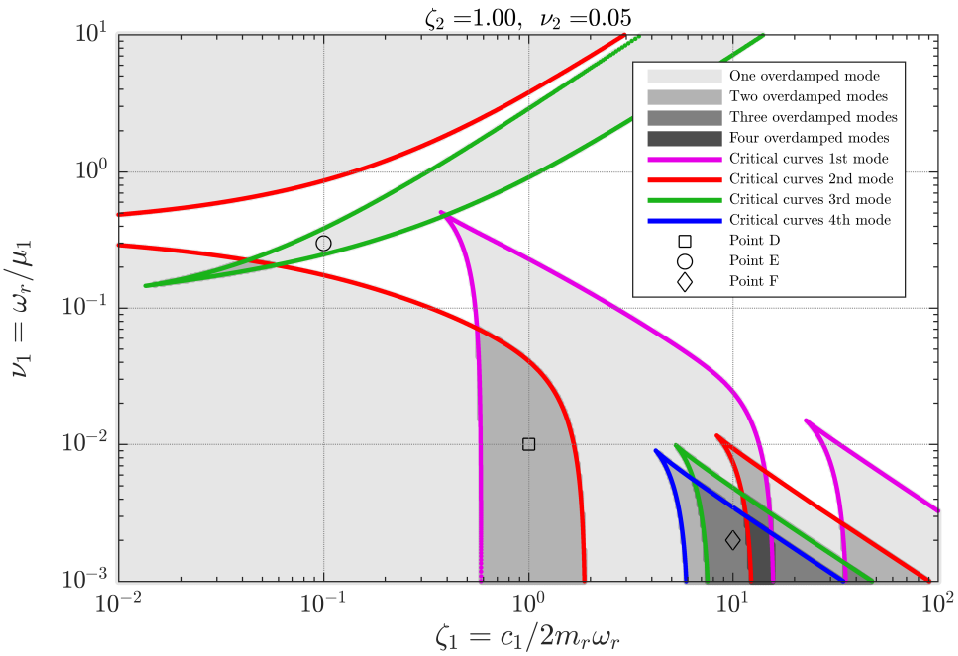

Figure 3: Example 1 (Case 2): Critical curves between nonviscous ratios $\zeta_1^{(j)}(\alpha)$ and $\nu_1^{(j)}(\alpha)$. Shaded region represents exact overdamped regions. The gray scale refers to the number of overdamped modes. Color curves (magenta,red,green and blue) represent the critical curves determined with the proposed method for the four modes $j = 1, 2, 3, 4$ respectively

modal viscous damping ratios depend on the damping parameters and, in addition, on the undamped natural frequencies as

$$Z_{1j} \equiv \frac{\boldsymbol{\phi}_j^T \mathbf{C}_1 \boldsymbol{\phi}_j}{2\omega_j} = \zeta \left(\frac{\omega_r}{\omega_j}\right) \tag{49}$$

$$Z_{2j} \equiv \frac{\boldsymbol{\phi}_j^T \mathbf{C}_2 \boldsymbol{\phi}_j}{2\omega_j} = \frac{\xi_0\,\omega_r + \lambda\,\xi_\infty\,\omega_j}{\omega_r + \lambda\,\omega_j} \tag{50}$$

In the current example it is observed that the ratios Z_{1j} are inversely proportional to the frequency since $\mathbf{C}_1$ is proportional to the mass matrix. While on the other hand, the model imposed for $\mathbf{C}_2$ enables the prediction of a constant modal ratio for high frequencies, say ξ_∞, and modal ratios close to ξ_0 for low frequencies. The transition between both ratios is achieved through a hyperbolic curve whose rate of change change is controlled by the parameter λ. In the Fig. 5, several examples of these modal ratios are shown graphically as a function of undamped natural frequencies.

The time and frequency dependency of the damping model is ruled by the two nonviscous coefficients, μ_1 and μ_2. In dimensionless form, the nonviscous ratios $\nu_1 = \omega_r/\mu_1$ and $\nu_2 = \omega_r/\mu_1$ are introduced. Therefore, the complete set of damping parameters for this example is

$$\{\nu_1,\ \nu_2,\ \zeta,\ \xi_0,\ \xi_\infty,\ \lambda\} \tag{51}$$

Equations (29) and (30) can be written as

$$\mathcal{R}_{1j}\,Z_{1j} + \mathcal{R}_{2j}\,Z_{2j} = U(\alpha) \tag{52}$$

$$\mathcal{R}_{1j}^2\,Z_{1j} + \mathcal{R}_{2j}^2\,Z_{2j} = V(\alpha) \tag{53}$$

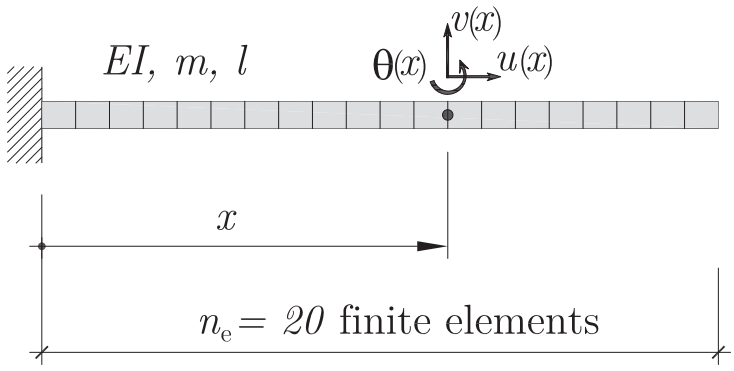

Figure 4: Example 2. A continuous system (beam) with 20 Euler-Bernouilli-type finite elements.

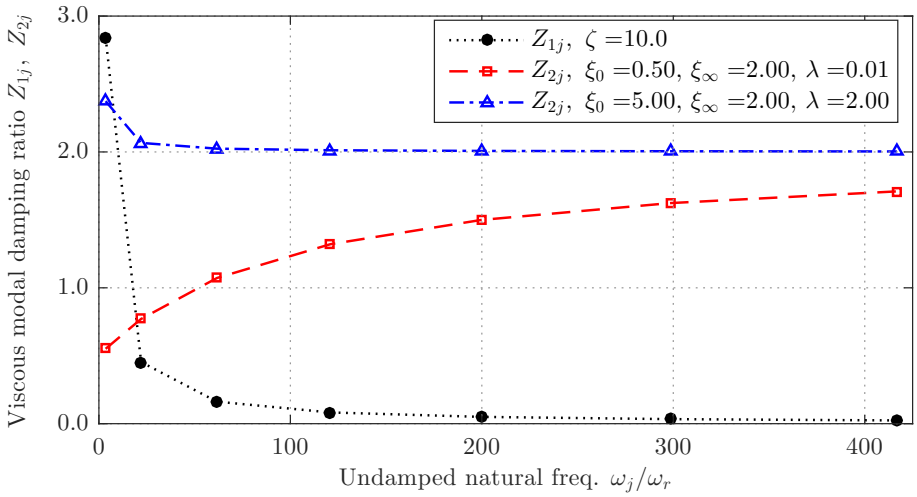

Figure 5: Example 2. Representation of the modal damping ratios vs the undamped natural frequences (seven modes, $1 \le j \le 7$): (i) Z_{1j}, black, Eq. (49), $\zeta = 10$; (ii) Z_{2j}, red, Eq. (49), $\xi_\infty = 2.0$, $\xi_0 = 0.50$, $\xi_\infty = 2.00$, $\lambda = 0.01$; (iii) Z_{2j}, blue, Eq. (49), $\xi_0 = 5.00$, $\xi_\infty = 2.00$, $\lambda = 2.00$

where

$$\mathcal{R}_{1j} = \frac{\alpha}{\alpha - \frac{\omega_j}{\omega_r}\nu_1}\ , \quad \mathcal{R}_{2j} = \frac{\alpha}{\alpha - \frac{\omega_j}{\omega_r}\nu_2}\ , \quad U = \frac{1+\alpha^2}{2\alpha}\ , \quad V = \frac{1}{\alpha} \tag{54}$$

The critical relationships between any pair of parameters are given analitically in parametric form solving the two Eqs. (52) and (53) as function of $\alpha \in (0, 1]$. In this example two cases will be studied:

- Case 3: critical curves between the viscous parameter of the 1st kernel, ζ, and one of the viscous parameters of the 2nd kernel, say ξ_0.

$$\{\zeta^{(j)}(\alpha), \xi_0^{(j)}(\alpha),\ 0 < \alpha \le 1,\ 1 \le j \le n\}$$

- Case 4: critical curves between the nonviscous parameter of the 1st kernel, ν_1 and one of the viscous parameters of the 2nd kernel, ξ_∞.

$$\{\xi_\infty^{(j)}(\alpha), \nu_1^{(j)}(\alpha)\ 0 < \alpha \le 1,\ 1 \le j \le n\}$$

.

In the Case 3, critical curves can be determined solving first for Z_{1j} and Z_{2j} in Eqs. (52) and (53).

$$Z_{1j}(\alpha) = \frac{\mathcal{R}_{2j}(\alpha)\,U(\alpha) - V(\alpha)}{\mathcal{R}_{1j}(\alpha)\,\left[\mathcal{R}_{2j}(\alpha) - \mathcal{R}_{1j}(\alpha)\right]}\ , \quad Z_{2j}(\alpha) = \frac{\mathcal{R}_{1j}(\alpha)\,U(\alpha) - V(\alpha)}{\mathcal{R}_{2j}(\alpha)\,\left[\mathcal{R}_{1j}(\alpha) - \mathcal{R}_{2j}(\alpha)\right]} \tag{55}$$

The parameters $\nu_1,\ \nu_2,\ \xi_\infty$ and λ must have been fixed previously. Using now Eqs. (49) and (50), both ζ and ξ_0 can be expressed just as function of α for each mode, yielding

$$\zeta^{(j)}(\alpha) = \left(\frac{\omega_j}{\omega_r}\right) Z_{1j}(\alpha)\ , \quad \xi_0^{(j)}(\alpha) = Z_{2j}(\alpha)\,\left[1 + \lambda\frac{\omega_j}{\omega_r}\right] - \lambda\,\xi_\infty\,\frac{\omega_j}{\omega_r}\ , \quad 1 \le j \le n \tag{56}$$

Evaluating the independent parameter α in the range $0 < \alpha \le 1$, the above expressions will provide the

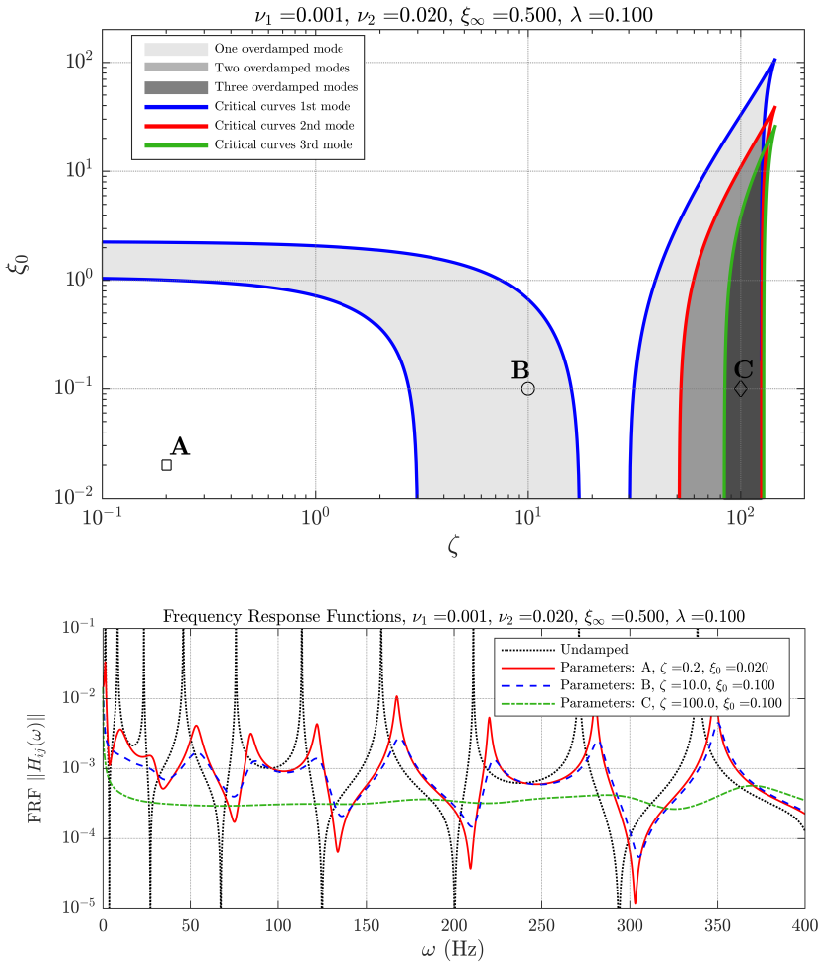

Figure 6: Example 2 (Case 3): [Top] Critical curves between viscous ratios ζ and ξ_0. Shaded region represents exact overdamped regions. The gray scale refers to the number of overdamped modes. Color curves (blue,red,green) depict the modal critical curves determined with the proposed method. [Bottom] Frequency Response Function in magnitude of degrees of freedom $(i, j) = (49, 60)$ obtained for the three shown points A, B and C.

exact set of critical points for the selected parameters. These values will have physical meaning if both are

positive. The curves obtained are shown in Fig. 6(top), where the figures arising present a similar structure to those of the previous example. These ones are curves that enclose regions that may overlap with each other. defining inner regions that indicate multiple overdamped modes. According to Ec. (49), the damping ratio of the higher modes decreases by the effect of the first kernel while it is tending to a constant value ξ_∞ by the effect of the second kernel. Thus, in this case of study, the highest modes will become overdamped provided that the parameter ζ takes very high values; as shown in the graph, values with the order of magnitude $\zeta \approx 100$. In order to note the effect of the damping parameters in the higher modes, several frequency response functions (FRF, magnitude) associated with the degrees of freedom $(i, j) = (49.60)$ have been plotted in Fig. 6(bottom). Point A lies in the underdamped region, leading to oscillatory modes. In low frequencies the effect of the first kernel through Z_{1j} is more important, such that the first modes become more damped. However, as the natural frequency increases, $Z_{1j} \approx 0$, while $Z_{2j} \approx 0.50$ (See Eqs. (49) and (49) for $\omega_j/\omega_r \gg 1$). According to the location of point C, the first three modes become overdamped. Althouth the level of damping is such that the oscillatory behaviour for higher modes has been almost completely lost.

In Case 4, the objective is to show critical relationships between the nonviscous parameter of the first kernel ν_1 and one of the viscous damping ratios of the second kernel, say ξ_∞. For that, Eqs (52) and (53) will be first resolved in the variables R_{1j} and Z_{2j}, because both carry independtly the parameters of study, ν_1 and ξ_∞, respectively. After some manipulations both equations can be transformed into the two quadratic polynomials

$$Z_{1j}\,\mathcal{R}_{1j}^2 - \mathcal{R}_{2j}\,Z_{1j}\,\mathcal{R}_{1j} + \mathcal{R}_{2j}\,U - V = 0 \tag{57}$$

$$\mathcal{R}_{2j}^2\,Z_{2j}^2 + (Z_{1j}\,\mathcal{R}_{2j} - 2U)\,\mathcal{R}_{2j}\,Z_{2j} + U^2 - Z_{1j}V = 0 \tag{58}$$

In the above equations the parameters ζ, ν_2, ξ_0 and λ are fixed and α is variable in the range $0 < \alpha \leq 1$. Z_{1j} and $\mathcal{R}_{2j}$ can be found in parametric form, allowing the analytical determination of ξ_∞ and ν_1 for each mode as

$$\xi_\infty^{(j)}(\alpha) = \frac{Z_{2j}(\alpha)(1 + \lambda\omega_j/\omega_r) - \xi_0}{\lambda\omega_j/\omega_r} \tag{59}$$

$$\nu_1^{(j)}(\alpha) = \alpha\frac{\mathcal{R}_{1j}(\alpha) - 1}{\mathcal{R}_{1j}(\alpha)}\,, \quad 1 \leq j \leq n \tag{60}$$

Fig. (7) shows the graph of the obtained curves together with the overdamped regions in gray-scaled colors, which have been drawn as described above. Certain region of the plot, approximately $0.8 \leq \xi_\infty \leq 1$, $0.001 \leq \nu_1 \leq 0.002$, corresponds to an overdamped region of the first four modes. Critical curve corresponding to the fifth mode (and highers) does not appear in Fig. (7) because the solution of Eqs. (59) and (60) does not correspond to values within the shown domain or even because there are no solutions compatible with the physically possible range of ξ_∞ and ν_1, that is $0 \leq \xi_\infty, \nu_1 < \infty$ with $\xi_\infty, \nu_1 \in \mathbb{R}$. As in the Case 3, the FRF in magnitude has been plotted for three different points in the parametric domain. Point A represents a highly damped condition althoug still with oscillatory nature. In fact, the relative maxima of the FRF-magnitude for point A corresponding to the (complex) resonance frequencies can still be noted, although only slightly.

It can also pointed out that, when several damping parameters come into play, the combination of these may result in regions where multiple modes are overdamped. It is not possible to predict a priori the ordering pattern of these regions and how they will combine with each other for the different modes. It is not even possible to know a priori whether for a particular value of the fixed parameters, others will present critical regions or not. Hence, the only way to properly answer these questions is by graphically displaying the regions.

The two numerical examples presented have highlighted the fact that tuning of damping parameters to control the modal overdamping or underdamping is possible. In the present work, systems subjected to a very strong energy dissipation are considered, with very high damping forces, in fact those necessary to

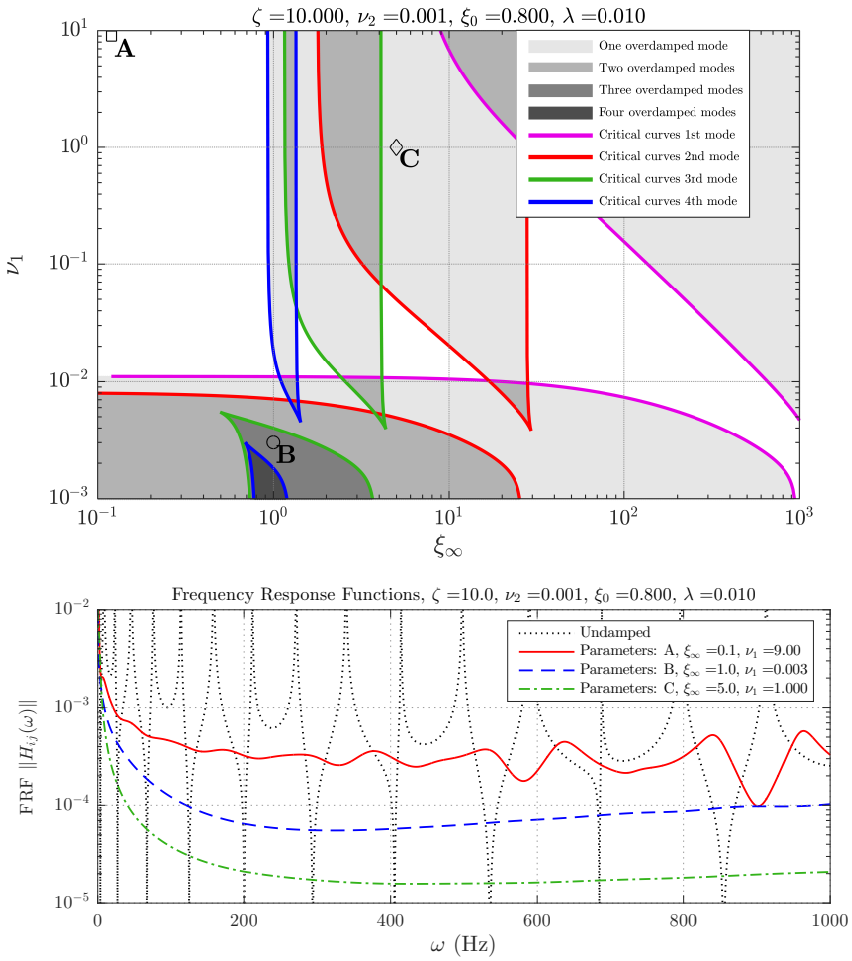

Figure 7: Example 2 (Case 4): [Top] Critical curves between viscous ratios ξ_∞ and ν_1. Shaded region represents exact overdamped regions. The gray scale refers to the number of overdamped modes. Color curves (magenta,red,green and blue) represent the critical curves determined with the proposed method for modes $j = 1, 2, 3, 4$ respectively. [Bottom] Frequency Response Function in magnitude of degrees of freedom $(i, j) = (49, 60)$ obtained for the three shown points A, B and C.

achieve overdamping in multiple modes. In structural dynamics the damping parameters are not generally considered as variables as done in this work but, on the contrary, are usually fixed by experimental results. It is not discussed that, possibly in some circumstances, there are no frequency-dependent materials or damping devices with values of parameters as those found by our approach. However, the aim of the paper is to present a general methodology that might even be valid for structured materials known in the literature as metamaterials [27].

It is known that entrees of mass and stiffness matrices have a close relation to mechanical and geometrical properties of the vibrating structure. However, damping parameters must be found mainly from modal identification analysis [28, 29]. However, certain sound absorption oscillators do have a relationship between their visco-thermal losses and the dimensions and characteristics [30]. We consider that the current methodology can have potential applications in the context of wave propagation and, in particular, in the design of new structures for perfect absorption. In fact, the extension of this theory is currently being studied for a direct relationship between the dimensions of the artificial resonators and the desired sound and vibration

effects, thus avoiding the use of inverse optimization tools carried out in recent works [31]. Additionally, the natural expansion to nonproportionally damped systems is also currently under research.

4. Conclusions

In this paper nonviscously damped multiple degree-of-freedom systems are considered. Nonviscous dissipative forces depend on the past history of the velocity response via convolution integrals over hereditary exponential kernels. The derivations of this paper have been carried out under the hypothesis of proportionally (or classically) damped structures. They are characterized by a damping matrix which becomes diagonal in the modal space of the undamped system. Determination of critical manifolds in viscoelastic systems consist of finding out the relationships between damping parameters for which some (or all) modes reach the overdamped state (lack of oscillatory motion). This article presents a general method to find the critical curves of any pair of parameters in systems with proportional damping. It is proved that the critical relationships can be obtained separately for each mode in parametric form. The proposal is validated throughout two numerical examples: the first one involving a 4-degree-of-freedom discrete system and the second one considering a continuous beam model with generalized proportional damping. Both examples show that, after the representation of the critical curves, the parametric domain is divided into regions where the modes are fully overdamped, something that is in agreement with the theoretical results. It follows that multiple modes may be overdamped in the areas resulting from the intersection of these regions.

Acknowledgments

This research was partially supported by the project HYPERMETA funded under the program Étoiles Montantes of the Région Pays de la Loire (France).

References

[1] S. Adhikari, Dynamics of non-viscously damped linear systems, J. Eng. Mech. 128 (3) (2002) 328–339.
[2] N. Wagner, S. Adhikari, Symmetric state-space method for a class of nonviscously damped systems, AIAA Journal 41 (5) (2003) 951–956.
[3] M. Lázaro, Nonviscous modes of nonproportionally damped viscoelastic systems, J. Appl. Mech. 82 (12) (2015) Art. 121011 (9 pp).
[4] M. Lázaro, Critical damping in non-viscously damped linear systems, Appl. Math. Modell. 65 (2019) 661–675.
[5] R. Duffin, A minimax theory for overdamped networks, J. Rat. Mech. Anal. 4 (2) (1955) 221–233.
[6] D. Nicholson, Eigenvalue bounds for damped linear systems, Mech. Res. Commun. 5 (3) (1978) 147–152.
[7] P. Muller, Oscillatory damped linear-systems, Mech. Res. Commun. 6 (2) (1979) 81–85.
[8] D. Inman, A. Andry, Some results on the nature of eigenvalues of discrete damped linear-systems, J. Appl. Mech. 47 (4) (1980) 927–930.
[9] L. Barkwell, P. Lancaster, Overdamped and Gyroscopic Vibrating Systems, J. Appl. Mech. 59 (1) (1992) 176–181.
[10] D. Beskos, B. Boley, Critical damping in linear discrete dynamic-systems, J. Appl. Mech. 47 (3) (1980) 627–630.
[11] S. Papargyri-Beskou, D. Beskos, On critical viscous damping determination in linear discrete dynamic systems, Acta Mech. 153 (1-2) (2002) 33–45.
[12] A. Muravyov, Forced vibration responses of viscoelastic structure, J. Sound Vib. 218 (5) (1998) 892–907.
[13] S. Adhikari, Qualitative dynamic characteristics of a non-viscously damped oscillator, Proc. R. Soc. London, Ser. A 461 (2059) (2005) 2269–2288.
[14] P. Muller, Are the eigensolutions of a l-d.o.f. system with viscoelastic damping oscillatory or not?, J. Sound Vib. 285 (1-2) (2005) 501–509.
[15] A. Muravyov, S. Hutton, Free vibration response characteristics of a simple elasto-hereditary system, J. Vib. Acoust. 120 (2) (1998) 628–632.
[16] M. Lázaro, Exact determination of critical damping in multiple-exponential-kernel based viscoelastic single degree-of-freedom systems, Math. Mech. Solids 24 (12) (2019) 3843–3861.
[17] E. Pierro, Damping control in viscoelastic beam dynamics, J. Vib. Control (in press)doi:10.1177/1077546320903195.
[18] P. Wang, Q. Wang, X. Xu, N. Chen, Fractional critical damping theory and its application in active suspension control, Shock Vib. 2017.
[19] M. Lázaro, Approximate critical curves in exponentially damped nonviscous systems, Mech. Syst. Sig. Process. 122 (2019) 720 – 736.
[20] L. Rayleigh, Theory of Sound, 2nd Edition, Dover Publications, 1945.

[21] T. Caughey, M. O'Kelly, Classical Normal Modes in Damped Linear Dynamic Systems, J. Appl. Mech. 32 (3) (1965) 583–588.
[22] S. Adhikari, Damping modelling using generalized proportional damping, J. Sound Vib. 293 (2006) 156–170.
[23] S. Adhikari, Classical normal modes in non-viscously damped linear systems, AIAA Journal 39 (5) (2001) 978–980.
[24] R. Lewandowski, M. Przychodzki, Approximate method for temperature-dependent characteristics of structures with viscoelastic dampers, Arch. Appl. Mech. 88 (10) (2018) 1695–1711.
[25] P. Litewka, R. Lewandowski, Dynamic characteristics of viscoelastic mindlin plates with influence of temperature, Comput. Struct. 229. (Art. 106181).
[26] M. Biot, Theory of stress-strain relations in anisotropic viscoelasticity and relaxation phenomena, J. Appl. Phys. 25 (11) (1954) 1385–1391.
[27] A. S. Phani, M. I. Hussein (Eds.), Dynamics of Lattice Materials, Willey, 2017.
[28] S. Adhikari, J. Woodhouse, Identification Of Damping: PART 1, Viscous Damping, J. Sound Vib. 243 (1) (2001) 43–61.
[29] S. Adhikari, J. Woodhouse, Identification Of Damping: PART 2, Non-Viscous Damping, J. Sound Vib. 243 (1) (2001) 63–88.
[30] M. Stinson, The propagation of plane sound waves in narrow and wide circular tubes, and generalization to uniform tubes of arbitrary cross-sectional shape, J. Acoust. Soc. Am.. 89 (2) (1991) 550–558.
[31] N. Jiménez, V. Romero-García, V. Pagneux, J.-P. Groby, Rainbow-trapping absorbers: Broadband, perfect and asymmetric sound absorption by subwavelength panels for transmission problems, Sci. Rep. 7 (1).